

# Some Au<sub>3</sub>Ru<sub>3</sub> clusters. X-ray structures of Ru<sub>3</sub>(μ<sub>3</sub>-CMeCHCMe)(CO)<sub>8</sub>{Au<sub>3</sub>(PPh<sub>3</sub>)<sub>3</sub>} and Ru<sub>3</sub>(μ<sub>3</sub>-C<sub>2</sub>Ph)(CO)<sub>8</sub>{Au<sub>3</sub>(PPh<sub>3</sub>)<sub>3</sub>}

Michael I. Bruce <sup>a</sup>, Paul A. Humphrey <sup>a</sup>, Brian W. Skelton <sup>b</sup>, Allan H. White <sup>b</sup>

<sup>a</sup> Jordan Laboratories, Department of Chemistry, University of Adelaide, Adelaide, SA 5005, South Australia

<sup>b</sup> Department of Chemistry, University of Western Australia, Nedlands, WA 6107, Western Australia

Received 14 February 1997

## Abstract

Several clusters containing Au<sub>3</sub>Ru<sub>3</sub> cores have been made from reactions between hydrido-triruthenium clusters or AuRu<sub>3</sub> clusters and [O{Au(PPh<sub>3</sub>)<sub>3</sub>}][BF<sub>4</sub>]. In the former case, the Au<sub>3</sub>(PPh<sub>3</sub>)<sub>3</sub> group acts as a three-electron donor, replacing (H + CO). The molecular structures of Ru<sub>3</sub>(μ<sub>3</sub>-CMeCHCMe)(CO)<sub>8</sub>{Au<sub>3</sub>(PPh<sub>3</sub>)<sub>3</sub>} (4) and Ru<sub>3</sub>(μ<sub>3</sub>-C<sub>2</sub>Ph)(CO)<sub>8</sub>{Au<sub>3</sub>(PPh<sub>3</sub>)<sub>3</sub>} (13) have been determined by X-ray crystallography. Comparisons are made between the parent Ru<sub>3</sub> clusters and their aured derivatives, which may contain open (bent) or closed triangular Au<sub>3</sub>P<sub>3</sub> moieties, according to whether there is more or less electron density on the cluster. © 1997 Elsevier Science S.A.

## 1. Introduction

Elsewhere we have described the use of the trigold-oxonium reagents [O{Au(PR<sub>3</sub>)<sub>3</sub>}]<sup>+</sup> (R = Ph, OMe) to introduce two Au(PR<sub>3</sub>) fragments into clusters in one step: with Ru<sub>3</sub> clusters, the tendency to form Au–Au bonds which is commonly found in polygold adducts of metal clusters resulted in the formation of a two-electron Au<sub>2</sub>(PR<sub>3</sub>)<sub>2</sub> unit which replaced either a CO group or two hydrogen atoms [1]. Formally, at least, the Au<sub>2</sub>(PPh<sub>3</sub>)<sub>2</sub> group is isolobal with the H<sub>2</sub> molecule, although detailed studies of the Au–Au interaction suggest that *d*<sup>2</sup>-*s* hybrid orbitals are used for Au–Au σ bonding with electron donation into empty 6*p* orbitals [2].

Subsequently we have found that more than two Au(PR<sub>3</sub>) groups may be introduced, as described herein. Previous examples of addition of three Au(PPh<sub>3</sub>) groups [or an Au<sub>3</sub>(PPh<sub>3</sub>)<sub>3</sub> moiety] are limited to reactions between polyhydrido clusters and AuMe(PPh<sub>3</sub>) [3a,3b] and the reactions of poly-anionic clusters with AuCl(PR<sub>3</sub>) [4] or [O{Au(PPh<sub>3</sub>)<sub>3</sub>}]<sup>+</sup> [5a,5b]. Trigold complexes containing only one other transition metal atom have been formed in reactions of hydrido derivatives with Au(NO<sub>3</sub>)(PPh<sub>3</sub>) [6]. The present method operates under mild conditions and illustrates a useful addition to the armoury of auring reagents. Part of this work has been communicated previously [7].

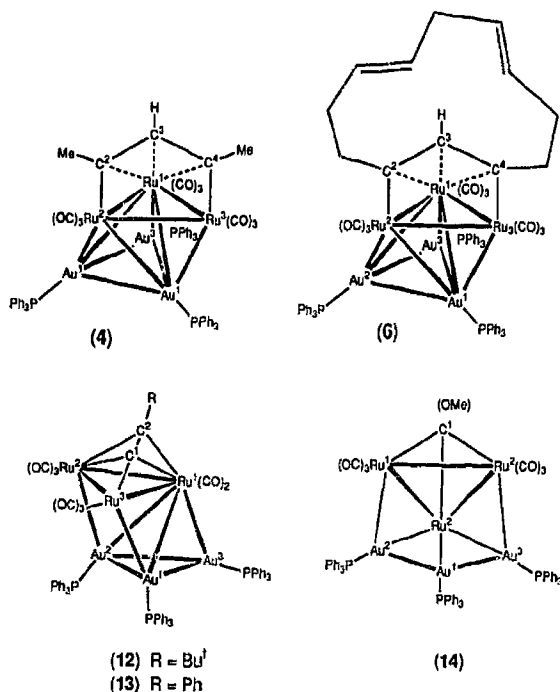
## 2. Results

The reactions described below were carried out in THF at room temperature and were generally complete within 15–30 min. The products were isolated by preparative t.l.c. and characterised by elemental microanalyses and from the usual spectroscopic properties where practicable. The most useful technique was fast atom bombardment (FAB) mass spectrometry, but as described before [8], ion association processes often resulted in the formation of aggregate ions containing extra Au or Au(PPh<sub>3</sub>) groups.

Reactions between Ru<sub>4</sub>(μ-H)<sub>4</sub>(CO)<sub>12</sub> and [O{Au(PPh<sub>3</sub>)<sub>3</sub>}]<sup>+</sup> in the presence of [ppn][Co(CO)<sub>4</sub>] ([ppn]<sup>+</sup> = [N(PPh<sub>3</sub>)<sub>2</sub>]<sup>+</sup>) afforded the known complexes Ru<sub>4</sub>(μ-H)<sub>4-n</sub>(CO)<sub>12</sub>{Au<sub>n</sub>(PPh<sub>3</sub>)<sub>n</sub>} [n = 1 (1), 3%; n = 2 (2), 33%; n = 3 (3), 2%]. Complex 3 was the sole product (59% yield) from reactions between Ru<sub>4</sub>(μ-H)<sub>4</sub>(CO)<sub>12</sub> and AuMe(PPh<sub>3</sub>) [3a,9], while all three complexes have been obtained from the various anions and AuCl(PPh<sub>3</sub>) or [O{Au(PPh<sub>3</sub>)<sub>3</sub>}]<sup>+</sup> [10]. The present method does not give a significantly increased yield of any of these products and shows that the use of the trigold-oxonium salt to replace H directly with Au(PPh<sub>3</sub>) is not an efficient route to these materials. The predominance of the Au<sub>2</sub>Ru<sub>4</sub> cluster serves to emphasise the role of the [Co(CO)<sub>4</sub>]<sup>−</sup> nucleophile in removing one of

the  $\text{Au}(\text{PPh}_3)$  units from the trigold-oxonium salt during the reaction [1].

In contrast, the cluster  $\text{Ru}_3(\mu_3\text{-CMeCHCMe})(\text{CO})_8\{\text{Au}_3(\text{PPh}_3)_3\}$  (**4**) was formed in virtually quantitative yield in the reaction between  $\text{Ru}_3(\mu\text{-H})(\mu_3\text{-CMeCHCMe})(\text{CO})_9$  [11], the trigold-oxonium salt and  $[\text{pph}][\text{Co}(\text{CO})_2]$ . Complex **4** was characterised by a rather imprecise single-crystal X-ray study (see below). The spectroscopic properties of **4** are generally in accord with the solid-state structure. In the IR spectrum, only four bands are found in the  $\nu(\text{CO})$  region between 2042 and 1914  $\text{cm}^{-1}$ . The  $^1\text{H}$  NMR spectrum contains resonances at  $\delta$  2.82 and 6.33, which can be assigned to the Me groups and the central H of the  $\mu_3$ -allylic ligand, respectively. At room temperature, the  $^{31}\text{P}$  NMR spectrum contains a broad resonance at  $\delta$  62.2, which at 245 K separates into two signals at  $\delta$  45.5 and 62.8 of relative intensities 1:2, respectively. This is not consistent with the solid-state structure (see below) where there are three types of  $\text{Au}(\text{PPh}_3)$  groups and suggests that at least two fluxional processes are occurring in solution, or that two of the expected singlet resonances are accidentally equivalent.



A similar reaction with  $\text{Ru}_3(\mu\text{-H})(\mu_3\text{-C}_{12}\text{H}_{15})(\text{CO})_9$  gave the two complexes  $\text{Ru}_3(\mu\text{-H})(\mu_3\text{-C}_{12}\text{H}_{15})(\text{CO})_8\{\text{Au}_2(\text{PPh}_3)_2\}$  (**5**; 60%) and  $\text{Ru}_3(\mu_3\text{-C}_{12}\text{H}_{15})(\text{CO})_8\{\text{Au}_3(\text{PPh}_3)_3\}$  (**6**; 29%). Complex **5** is new and was characterised by elemental analysis and from its FAB mass spectrum. As with other complexes derived from 1,5,9-cyclododecatriene, the  $^1\text{H}$  NMR spectrum is complex, containing several overlapping reso-

nances for the ring protons. However, the  $\text{Ru-H}$  resonance at  $\delta$  -21.15 and the central allylic proton at  $\delta$  6.39, which are coupled to each other [ $J(\text{HH}) = 2.3$  Hz] are characteristic of these complexes [12].

Complex **6** has been prepared on an earlier occasion, by deprotonation of the parent  $\text{Ru}_3$  cluster with  $\text{K-Selectride}$  ( $\text{K}[\text{BHBu}_3^s]$ ) and addition of  $[\text{O}(\text{Au}(\text{PPh}_3))_3]^+$ ; its structure was determined by X-ray crystallography [13]. The  $^{31}\text{P}$  NMR spectrum of **6** contains a singlet at  $\delta$  60.3 at room temperature. On cooling to 245 K, this separates into three equal intensity signals at  $\delta$  46.2, 61.7 and 64.5, in accord with the solid-state structure, which has three non-equivalent  $\text{Au}(\text{PPh}_3)$  groups.

Partially auroated hydrido-ruthenium clusters can exchange further hydrogens for  $\text{Au}(\text{PR}_3)$  groups. For example, the reaction between  $\text{Ru}_4(\mu_3\text{-H})_2(\text{CO})_{12}\{\text{Au}_2(\text{PPh}_3)_2\}$  and  $\text{AuMe}(\text{PPh}_3)$  gave a 63% yield of **3**, while  $\text{Ru}_4(\mu_3\text{-H})_2(\text{CO})_{12}\{\text{Au}_2(\mu\text{-dppm})\}$  similarly gave  $\text{Ru}_4(\mu\text{-H})(\text{CO})_{12}\{\text{Au}_3(\mu\text{-dppm})(\text{PPh}_3)\}$  (**7**) (54%) [9]. Here we have investigated the further addition of  $\text{Au}(\text{PPh}_3)$  groups to clusters already containing one gold atom but no hydride. The complex  $\text{Ru}_3(\mu_3\text{-C}_2\text{Bu}^1)(\text{CO})_9\{\text{Au}(\text{PPh}_3)\}$  (**8**) was originally described by Braunstein and coworkers [14], who also determined its structure. An alternative, improved, synthesis of this complex, and the related derivatives  $\text{Ru}_3(\mu_3\text{-C}_2\text{Ph})(\text{CO})_9\{\text{Au}(\text{L})\}$  [ $\text{L} = \text{PPh}_3$  (**9**),  $\text{P}(\text{tol})_3$  (**10**)] and  $\{\text{Ru}_3(\mu_3\text{-F}_2\text{Ph})(\text{CO})_9\text{Au}_2(\mu\text{-dppe})\}$  (**11**), by direct addition of  $\text{Au}(\text{C}_2\text{R})(\text{L})$  to  $\text{Ru}_3(\text{CO})_{12}$  in the presence of  $\text{Me}_3\text{NO}$ , is described in the Section 5. The reaction between **8** and the trigold-oxonium salt gave

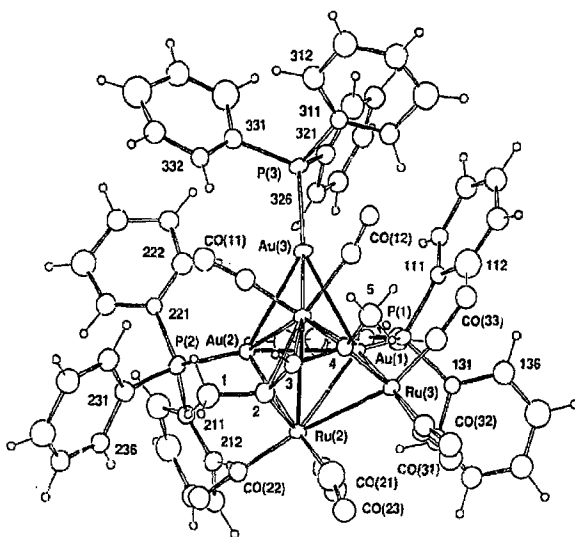


Fig. 1. Plot of a molecule of  $\text{Ru}_3(\mu_3\text{-CMeCHCMe})(\text{CO})_8\{\text{Au}_3(\text{PPh}_3)_3\}$  (**4**), onto the  $\text{Au}_3$  plane, showing the atom numbering scheme, carbon atoms being designated by number only. Non-hydrogen atoms are shown with 20% thermal envelopes; hydrogen atoms have arbitrary radii of 0.1 Å.

Table 1  
Selected structural parameters in  $\text{Au}_3\text{Ru}_3$  and  $\text{Au}_3\text{Ru}_2\text{Co}$  complexes compared with analogous  $\text{Ru}_3$  complexes (see also Fig. 3)

(i) Type (a)							
Complex	3	14	15	19	7		
Reference	10	3	3b	5a	22		
Core	Au <sub>3</sub> Ru <sub>3</sub>	Au <sub>3</sub> Ru <sub>3</sub>	AuRu <sub>3</sub>	Au <sub>3</sub> Ru <sub>2</sub> Co	Au <sub>3</sub> Ru <sub>3</sub>		
Au(1)–Au(2)	2.838(1)	3.010(1)	2.836(1)	2.749(2)			
Au(1)–Au(3)	2.835(1)	2.930(1)	2.784(1)	2.758(2)			
Au(2)–Au(3)	[4.809(3)]	[4.81]*	[4.73]*	[4.659(2)]			
Au(1)–Ru(1)	2.838(2)	2.987(2)	2.727(1)	2.850(2)	2.920(3)		
Au(1)–Ru(2)	3.007(2)	2.818(2)	2.879(1)	2.726(4) [Co]	2.779(3)		
Au(1)–Ru(3)	2.972(2)	2.825(2)	2.763(1)	3.054(3)	[3.546(3)]		
Au(2)–Ru(1)	2.837(2)	2.844(2)	2.813(2)	2.812(3)			
Au(2)–Ru(2)	2.850(2)	2.807(2)	2.712(4) [Co]	2.895(3)			
Au(3)–Ru(1)	2.840(2)	2.833(2)	2.783(2)	2.762(3)			
Au(3)–Ru(3)	2.821(2)	2.796(2)	2.917(3)	2.867(3)			
Ru(1)–Ru(2)	2.979(2)	2.913(2)	2.875(2)	2.825(4) [Co]	3.043(3)		
Ru(1)–Ru(3)	3.004(3)	2.929(2)	2.879(2)	2.992(3)	2.965(4)		
Ru(2)–Ru(3)	2.968(3)	2.895(2)	2.865(2)	2.710(3) [Co]	2.839(4)		
Ru–Ru (av.)	2.98 <sub>4</sub>	2.91 <sub>2</sub>	2.873		2.95		
Δ(Ru–Ru)		0.039					
Au(2)–Au(1)–Au(3)	115.9(1)	108.0 *		114.7 *	115.6(1)		
Au(2)–Ru(1)–Au(3)	115.8(1)	115.7 *		115.5 *	113.4(1)		
Dihedral Au <sub>3</sub> /Ru <sub>3</sub>	37.20(1)	29.47 *		84.66 *	48.52(9)		
(ii) Type (b)							
Complex	4	18	13	8	17	6	16
Reference	This work	20	This work	14	19	13	18
Core	Au <sub>3</sub> Ru <sub>3</sub>	Ru <sub>3</sub>	Au <sub>3</sub> Ru <sub>3</sub>	AuRu <sub>3</sub>	Ru <sub>3</sub>	Au <sub>3</sub> Ru <sub>3</sub>	Ru <sub>3</sub>
Au(1)–Au(2)	2.893(3)		2.911(2)			2.911(3)	
Au(1)–Au(3)	2.848(2)		2.809(2)			2.865(2)	
Au(2)–Au(3)	2.849(2)		2.899(2)			2.840(2)	
Au(1)–Ru(1)	2.790(4)		2.707(2)	2.757(1)		2.737(3)	
Au(1)–Ru(2)	2.962(4)		4.197(2)	2.763(1)		2.943(4)	
Au(1)–Ru(3)	2.855(5)		2.868(2)			2.896(4)	
Au(2)–Ru(1)	2.792(4)		2.674(2)			2.775(4)	
Au(2)–Ru(2)	2.879(4)		2.919(2)			2.882(4)	
Au(3)–Ru(1)	2.750(5)		2.721(2)			2.761(3)	
Ru(1)–Ru(2)	2.921(4)	2.777(2)	2.776(2)	2.820(1)	2.792(3)	2.922(4)	2.929(4)
Ru(1)–Ru(3)	2.955(4)	2.777(2)	2.971(3)	2.800(1)	2.799(3)	2.929(5)	2.779(4)
Ru(2)–Ru(3)	2.845(5)	2.933(2)	2.844(2)	2.786(1)	2.795(3)	2.845(5)	2.775(4)
Ru–Ru (av.)	2.907	2.829	2.864	2.802	2.795	2.898	2.828
Δ(Ru–Ru)	0.078		0.069			0.070	
Dihedral Au <sub>3</sub> /Ru <sub>3</sub>	20.69(9)		8.87(4)			23.0(2)	

\* Original atom numbering has been altered in some cases for consistency; for compounds with asterisked entries, there is no Cambridge Data Base coordinate record, precluding estimates of precision for these entries. Non-bonded distances are in square brackets.

Table 2  
Comparison of Au–P and Ru–organic ligand bond lengths in  $\text{Au}_3\text{P}_3$  complexes and precursor complexes

Complex	4	18	13	8	17	6	16
Reference	This work	20	This work	14	19	13	18
Au(1)–P(1)	2.30(1)		2.299(4)	2.276(3)		2.31(1)	
Au(2)–P(2)	2.313(9)		2.299(5)			2.26(1)	
Au(3)–P(3)	2.294(8)		2.282(4)			2.22(2)	
Ru(1)–C(1)			2.15(1)	2.22(1)	2.214(3)		2.02(3)
Ru(1)–C(2)	2.28(3)	2.250(8)	2.19(1)	2.21(1)	2.271(3)	2.22(5)	2.18(3)
Ru(1)–C(3)	2.22(3)	2.333(8)				2.23(4)	2.19(3)
Ru(1)–C(4)	2.19(3)	2.250(8)				2.11(4)	2.23(3)
Ru(2)–C(1)			2.20(2)	2.19(1)	2.207(3)		
Ru(2)–C(2)	2.02(3)	2.088(6)	2.21(2)	2.27(1)	2.268(3)	2.05(4)	
Ru(3)–C(1)			1.95(1)	1.95(2)	1.947(3)		
Ru(3)–C(4)	2.12(3)	2.088(6)				2.14(1)	2.01(3)
For 4:	Au(1)–C(31) 2.85(3), Au(2)–C(11) 2.95(4), Au(3)–C(11) 2.87(4), Au(3)–C(12) 2.76(4) Å						
For 13:	Au(2)–C(21) 2.80(1), Au(3)–C(11) 2.78(2) Å.						

Original atom numbering has been altered in some cases for consistency. See also Fig. 3.

orange  $\text{Ru}_3(\mu_3\text{-C}_2\text{Bu}^i)(\text{CO})_8\{\text{Au}_3(\text{PPh}_3)_3\}$  (**12**) in 74% yield. The phenyl analogue,  $\text{Ru}_3(\mu_3\text{-C}_2\text{Ph})(\text{CO})_8\{\text{Au}_3(\text{PPh}_3)_3\}$  (**13**), was obtained (75%) in similar fashion. Complex **12** has been previously isolated from reactions between  $[\text{O}(\text{Au}(\text{PPh}_3))_3][\text{BF}_4]$  and the anion  $[\text{Ru}_3(\mu_3\text{-C}_2\text{Bu}^i)(\text{CO})_9]^-$  in 3% yield, the major product being the vinylidene cluster  $\text{Ru}_3(\mu_3\text{-C}=\text{CHBu}^i)(\text{CO})_9\{\text{Au}_2(\text{PPh}_3)_2\}$  [15]. The molecular structure of **13** was determined by X-ray crystallography and is described below.

The IR spectra contained four strong terminal  $\nu(\text{CO})$  bands; the expected resonances for Ph, and Bu<sup>i</sup> groups if present, appeared in the <sup>1</sup>H NMR spectra of the two complexes. At room temperature, only a single broad resonance is found at  $\delta$  56.7 in the <sup>31</sup>P NMR spectrum of **13**. On cooling to 255 K, three singlets are found between  $\delta$  51.7 and 65.3, again consistent with the solid-state structure.

## 2.1. Molecular structures

### 2.1.1. $\text{Ru}_3(\mu_3\text{-CMeCHCMe})(\text{CO})_8\{\text{Au}_3(\text{PPh}_3)_3\}$ (**4**)

A plot of a molecule of **4** is shown in Fig. 1 and selected structural parameters are given in Tables 1 and 2. The metal core consists of the original  $\text{Ru}_3$  cluster [ $\text{Ru-Ru}$  2.845(5)–2.955(4) Å] to which a closed triangular  $\text{Au}_3$  unit [ $\text{Au-Au}$  2.848(2)–2.893(3) Å] is attached by six metal–metal bonds [ $\text{Au-Ru}$  2.750(5)–2.962(4) Å] to form a face-capped trigonal bipyramid. The organic ligand is attached to the  $\text{Ru}_3$  face furthest from the  $\text{Au}_3$  face, and almost parallel to it, in the same  $\eta^1:\eta^1:\eta^3$  fashion as found in the parent complex. The five carbon atoms are coplanar ( $\chi^2 = 11$ ), the interplanar dihedral angles to the  $\text{Ru}_3$  and  $\text{Au}_3$  planes being

54(2), 60(2)°. Eight terminal CO ligands are attached to the three ruthenium atoms, while each gold atom bears a  $\text{PPh}_3$  ligand [ $\text{Au-P}$  2.294(8)–2.313(9) Å; atoms P(1–3) lie out of the  $\text{Au}_3$  plane by 1.93(1), 1.35(1) and 0.91(1) Å.

### 2.1.2. $\text{Ru}_3(\mu_3\text{-C}_2\text{Ph})(\text{CO})_8\{\text{Au}_3(\text{PPh}_3)_3\}$ (**13**)

The molecular structure of **13** is shown in Fig. 2 with selected bond lengths and angles being presented in Tables 1 and 2. The metal core is similar to that found in **4**, but interaction of the  $\text{Au}_3$  unit [ $\text{Au-Au}$  2.809(2)–2.911(2) Å] with the  $\text{Ru}_3$  cluster [ $\text{Ru-Ru}$  2.776(2)–2.971(3) Å] via only five  $\text{Au-Ru}$  bonds [ $\text{Au-Ru}$  2.674(2)–2.919(2) Å] results in distortion of the  $\text{Au}_3\text{Ru}_3$  cluster towards a capped square pyramid. The organic ligand is found on the face of the  $\text{Ru}_3$  triangle opposite to the  $\text{Au}_3(\text{PPh}_3)_3$  unit, with the  $\sigma$ -bonded carbon being attached to a basal ruthenium of the square pyramid; atoms C(1,2) deviate from the  $\text{Ru}_3$  plane by 1.27(2), 1.70(2) Å. Eight terminal CO ligands are attached to the ruthenium atoms and each gold atom is bonded to a  $\text{PPh}_3$  ligand [ $\text{Au-P}$  2.282–2.299(4) Å], atoms P(1–3) lying out of the  $\text{Au}_3$  plane by 1.678(4), 1.900(5), 0.798(5) Å.

In both structures, relatively close approaches of the gold atoms to one or more CO groups [2.76–2.97 Å] are found. Similar observations have been recorded for other gold-containing clusters, such as  $\text{Os}_{10}\text{C}(\text{CO})_{24}\{\text{Au}_4(\text{PCy}_3)_3\}$ , in which  $\text{Au}\cdots\text{C}$  separations of 2.66–2.76 Å were noted [16].

## 3. Discussion

We have described above a useful extension of the previous study [1] of reactions of ruthenium cluster complexes with  $[\text{O}(\text{Au}(\text{PPh}_3))_3]^+$  which leads to a method of introducing three  $\text{Au}(\text{PPh}_3)$  groups into metal clusters. The reactions proceed readily under ambient conditions to give moderate to high yields of the products.

With the present work, there are now structural data for seven cluster complexes containing  $\text{Au}_3(\text{PR}_3)_3$  attached to triangular faces of  $\text{Ru}_3$ ,  $\text{Ru}_4$  or, in one case,  $\text{Ru}_3\text{Co}$ , cores. In all but one case, the phosphine is  $\text{PPh}_3$ ; the exception (**7**) contains an  $\text{Au}_3(\text{PPh}_3)(\mu\text{-dppm})$ . Structural data are also available for their direct precursors or for closely related complexes in four instances. It is thus possible to consider the geometries of the various  $\text{Au}_3(\text{PR}_3)_3$  groups and the effects of adding the  $\text{Au}_3(\text{PR}_3)_3$  group to the  $\text{Ru}_3$  cluster. Relevant structural parameters are collected in Table 1 for the following complexes:  $\text{Ru}_3\{\mu\text{-C}(\text{OMe})(\text{CO})_9\{\text{Au}_3(\text{PPh}_3)_3\}\}$  (**14**) [3b],  $\text{Ru}_3(\mu\text{-H})_2\{\mu_3\text{-C}(\text{OMe})(\text{CO})_9\{\text{Au}(\text{PPh}_3)\}\}$  (**15**) [3b] [the precursor in this case is  $\text{Ru}_3(\mu\text{-H})\{\mu\text{-C}(\text{OMe})(\text{CO})_{10}\}$  [17]]; **6** and

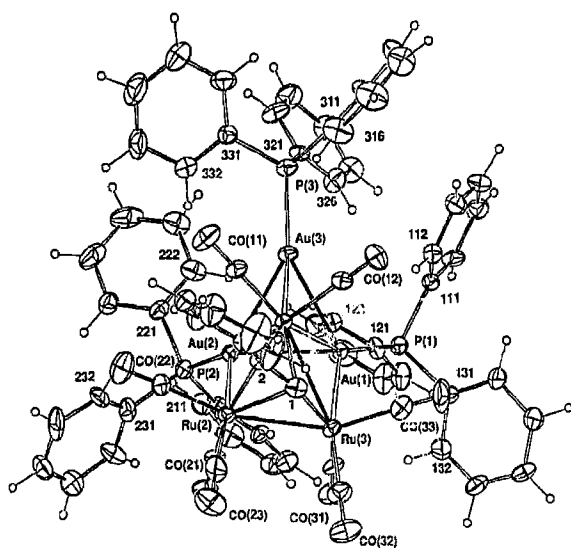


Fig. 2. Plot of a molecule of  $\text{Ru}_3(\mu_3\text{-C}_2\text{Ph})(\text{CO})_8\{\text{Au}_3(\text{PPh}_3)_3\}$  (**13**), showing the atom numbering scheme. Non-hydrogen atoms are shown with 20% thermal envelopes; hydrogen atoms have arbitrary radii of 0.1 Å.

$\text{Ru}_3(\mu\text{-H})(\mu\text{-C}_{12}\text{H}_{15})(\text{CO})_9$  (**16**) [18]; **13** and  $\text{Ru}_3(\mu\text{-X})(\mu_3\text{-C}_2\text{Bu}^t)(\text{CO})_9$  [ $\text{X} = \text{H}$  (**17**) [19],  $\text{Au}(\text{PPh}_3)$  (**8**) [14]]; **4** and  $\text{Ru}_3(\mu\text{-H})(\mu_3\text{-CMeCMeCMe})(\text{CO})_9$  (**18**) [20]; **3**, **7** and  $\text{Ru}_3\text{Co}(\text{CO})_{12}(\text{Au}_3(\text{PPh}_3)_3)$  (**19**) [5a]. Fig. 3 contains plots of the  $\text{Au}_3\text{Ru}_3$  ( $\text{Au}_3\text{Ru}_2\text{Co}$  for **19**) cores of the seven complexes.

### 3.1. The $\text{Au}_3(\text{PR}_3)_3$ ligand

From Fig. 3, it can be seen that there are several examples of each of two geometries of the  $\text{Au}_3(\text{PPh}_3)_3$  group in these clusters: (a) an open (bent)  $\text{Au}_3$  unit spanning an Ru–Ru bond, as found in **3**, **7** and **14** and in **19**, where it is attached to an  $\text{Ru}_2\text{Co}$  face [5a] and (b) a closed triangular  $\text{Au}_3$  unit strongly attached to a single Ru atom of the cluster, with weaker interactions with adjacent Ru atoms (as found in **4**, **6** and **13**). The two forms are formally obtained (a) by the first  $\text{Au}(\text{PR}_3)_3$  group capping an  $\text{Ru}_3$  face, followed by the other  $\text{Au}(\text{PR}_3)_3$  groups capping opposite  $\text{AuRu}_2$  faces, and (b) by successive capping of  $\text{Ru}_3$ ,  $\text{AuRu}_2$  and  $\text{Au}_2\text{Ru}$  faces. In  $\text{Ru}_4(\mu\text{-H})(\text{CO})_{12}\{\text{Au}_3(\mu\text{-dppm})(\text{PPh}_3)\}$  (**7**) [21], the  $\text{Au}_3\text{Ru}_4$  cluster is formed from a square-pyramidal  $\text{Ru}_3\text{Au}_3$  core (with a square  $\text{Au}_2\text{Ru}_2$  face) capped on the  $\text{Ru}_3$  face by the fourth  $\text{Ru}(\text{CO})_3$  group. This appears to be a distorted version of type (a), probably resulting from the presence of the small bite ligand dppm bridging two of the Au atoms. The steric constraints thus imposed have pulled  $\text{Au}(1)$  away from  $\text{Ru}(3)$  [3.55 Å] to give a bent  $\text{Au}_2\text{Ru}_2$  rhomboid.

Within the  $\text{Au}_3$  unit, type (a) has two bonding Au–Au interactions [2.75–3.01 Å]; the  $\text{Au}(2)\dots\text{Au}(3)$  separations range between 4.73 and 4.81 Å and are clearly non-bonding. The two outer  $\text{Au}(2,3)$  atoms have Au–

$\text{Ru}(1)$  contacts of 2.76–2.84 Å, and are somewhat further away from the other two Ru atoms [2.80–2.92 Å]. Atom  $\text{Au}(1)$  is found either ca. 2.81 (**14**) or 2.97–3.02 Å (**3**, **7** and **19**) from  $\text{Ru}(2,3)$ . In **7**, a close approach to  $\text{Ru}(2)$  (2.78 Å) is balanced by a long non-bonding separation from  $\text{Ru}(3)$  (3.55 Å). The Au–Au–Au angles are ca. 110°, even in **7** [115.6(1)°; cf. 115.9(1)° in the closely related complex **3**] [3a,3b,9].

For type (b), the  $\text{Au}_3$  triangle (Au–Au 2.81–2.91 Å) strongly interacts with  $\text{Ru}(1)$  (2.67–2.79 Å). Atoms  $\text{Au}(1,2)$  are located above the  $\text{Ru}(1)\text{--Ru}(2)$  and  $\text{Ru}(1)\text{--Ru}(3)$  vectors, respectively, with  $\text{Au}(1)\text{--Ru}(2,3)$  and  $\text{Au}(2)\text{--Ru}(2)$  distances of 2.86–2.96 Å. In both cases, the Au–Au distances span those found in gold metal (2.884 Å) [22], but even in complexes which are otherwise symmetrical, presently inexplicable differences in the Au–Au separations are found, e.g. in **14**, where values of 2.930(1) and 3.010(1) Å were found [3b]. In all cases mentioned the Au atoms are close enough for there to be considerable bonding interactions.

### 3.2. Effect of addition of $\text{Au}_3\text{P}_3$ to the $\text{Ru}_3$ face

As has been noted before [1,3b], addition of  $\text{Au}(\text{PR}_3)_3$  units to an  $\text{Ru}_3$  face of a cluster complex has the effect of increasing the average Ru–Ru separations. Thus for the ‘‘parent’’ complexes considered here, the average Ru–Ru bond lengths range from 2.795 to 2.873 Å (see Table 1), while in the  $\text{Au}_3\text{Ru}_3$  clusters, the values have increased to between 2.864 and 2.912 Å. In cases where individual Ru–Ru separations are not changed significantly, these bonds are usually bridged by another ligand, such as H or C(OMe).

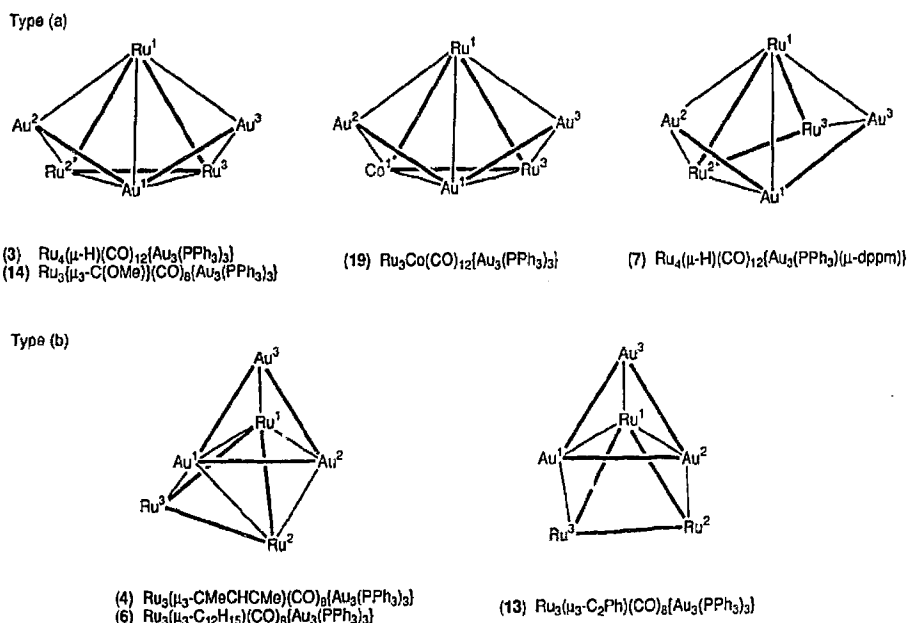


Fig. 3. Plots of the  $\text{Au}_3\text{Ru}_3$  or  $\text{Au}_3\text{Ru}_2\text{Co}$  cores of several cluster complexes.

Where replacement of one H by  $\text{Au}(\text{PPh}_3)$  occurs there is only a slight increase in average Ru–Ru separation (2.795 to 2.802 Å), although individual Ru–Ru separations have a wider range in **8** (between 2.786 and 2.820 Å), compared with 2.792–2.795 Å in **17**. Further addition of the  $\text{Au}_2(\text{PPh}_3)_2$  fragment to a complex already containing an  $\text{Au}(\text{PPh}_3)$  group results in an additional expansion of the average Ru–Ru separation, e.g. comparing **8** with **13**, from 2.802 to 2.864 Å. The changes in average Ru–Ru separation [ $\Delta(\text{Ru–Ru})$ ] range between 0.04 and 0.08 Å in the pairs **4/18**, **13/17**, **14/15** and **6/16**; consideration of the pairs **8/13** and **14/15** and the minimal expansion found for **8/17**, suggest that it is the addition of the second and third  $\text{Au}(\text{PR}_3)$  groups that results in the cluster expansion.

Of some interest is the finding that the  $\text{Au}_3/\text{Ru}_3$  interplanar angles are markedly different in the two types, ranging from 29.47–48.52° (largest value for **7**) in type (a) and 8.87–23.03° in type (b), although in the  $\text{Ru}_2\text{Co}$  complex **19**, the two planes diverge by 84.66°.

### 3.3. Electronic effect of the $\text{Au}_3\text{P}_3$ group

Comparisons of the bonding of the organic ligand in complexes **4/18** and **8/13/17** (Table 2) show relatively minor changes occur on auration, with perhaps a trend towards a closer attachment in the case of the  $\text{Au}_3\text{Ru}_3$  complexes. The observed expansion can be rationalised, as before [1], by the increased size of the  $\text{Au}_3(\text{PR}_3)_3$  group as well as by the presence of a more electron-donating group replacing the H atom or CO group. The  $\nu(\text{CO})$  frequencies of the  $\text{Au}_3\text{Ru}_3$  complexes are some 20–30  $\text{cm}^{-1}$  less than those found for the parent complexes, which is also consistent with the presence of increased electron densities in the aured clusters. In turn, this would result in increased back-bonding to the  $\pi$ -bound part of the ligand. There is no significant observable effect on the Ru–C  $\sigma$ -bonds and the geometries of the ligand fragments are essentially unchanged.

### 3.4. Isolobal matters

The molecular structures of the products described above and others show that the three  $\text{Au}(\text{PR}_3)$  groups are generally linked by Au–Au bonds, a phenomenon which has been termed ‘‘aurophilicity’’ [23]. Consequently, the well-known isolobal relationship between  $[\text{Au}(\text{PR}_3)]^+$  and  $\text{H}^+$  [24] does not hold in these clusters. In polyhydrido clusters the H atoms are generally found to bridge separate edges or cap separate faces. For example, in  $\text{Ru}_4(\mu\text{-H})_4(\text{CO})_{12}$ , the H atoms are found to bridge Ru–Ru edges, while the gold atom similarly bridges an Ru–Ru edge in the mono- $\text{Au}(\text{PR}_3)$  derivative **1** [25]. However, energy differences between  $\mu_2$ - and  $\mu_3$ -groups are small, so that the solid-state struc-

tures probably reflect arrangements of minimum energy. For example, two isomers of  $\text{AuRu}_5\text{C}(\text{CO})_{13}(\text{NO})(\text{PEt}_3)$  are known, in which the  $\text{Au}(\text{PEt}_3)$  unit either bridges an Ru–Ru edge or caps an  $\text{Ru}_3$  face [26].

If two gold atoms are present, as in **2**, the second  $\text{Au}(\text{PR}_3)$  moiety caps an  $\text{AuRu}_2$  face, so that Au–Au bonds are formed [27]. The formal isolobal analogues of these complexes would be cluster complexes of molecular  $\text{H}_2$ , but so far none have been identified, although their mononuclear counterparts have been known since 1984 [28].

In the present context, if the H/ $\text{Au}(\text{PR}_3)$  analogy is pursued, the formal isolobal relationship is between  $[\text{Au}_3(\text{PPh}_3)_3]^+$  and  $\text{H}_3^+$ . The structure of the ground state of  $\text{H}_3^+$  has been calculated to have a closed triangular arrangement of the three H atoms [analogous to the type (b)  $\text{Au}_3(\text{PR}_3)_3$  group] [29]. In contrast, calculations of the geometry of  $\text{H}_3$  ligands on  $\text{Cr}(\text{CO})_5$  indicate that the open (bent) geometry, analogous to type (a)  $\text{Au}_3(\text{PR}_3)_3$ , is energetically more favourable [30]. Some justification of this lies in the fact that the 2-e cyclic  $\text{H}_3^+$  moiety is stable, but Jahn–Teller distortions lead to separation of two of the H atoms to give the open (bent) form as more electron density is added. Interestingly, three  $\text{Au}(\text{PR}_3)$  units have also been added to mononuclear complexes and it is of interest that in one case, at least, a skeletal rearrangement of the open  $\text{Au}_3(\text{PPh}_3)_3$  portion found in  $\text{ReH}_2(\text{PMe}_2\text{Ph})_3\{\text{Au}_3(\text{PPh}_3)_3\}$ , i.e., with a butterfly  $\text{Au}_3\text{Re}$  cluster, to the closed form occurs on protonation. In the resulting cation  $[\text{ReH}_3(\text{PMe}_2\text{Ph})_3\{\text{Au}_3(\text{PPh}_3)_3\}]^+$ , the  $\text{Au}_3\text{Re}$  core is tetrahedral [31]. Thus an increase in electron density results in opening of the  $\text{Au}_3$  triangle, paralleling the behaviour of the  $\text{H}_3^+$  moiety.

### 3.5. Fluxional behaviour

Polygold–ruthenium clusters are often found to be fluxional via variable temperature  $^{31}\text{P}$  NMR studies. Detailed studies of several complexes, including those containing type (a)  $\text{Au}_3(\text{PR}_3)_3$  groups, suggest that the mechanism whereby the P atoms of the tertiary phosphines achieve equivalence is a polyhedral rearrangement during which Au–Au bonds are cleaved and reformed [32]. Studies of the fluxional behaviour of **7** in solution have provided further information about these processes [32].

Singlet  $^{31}\text{P}$  resonances were found for **4**, **6** and **13** at room temperature, which on cooling to ca. 250 K separate into two (**4**) or three peaks (**6** and **13**). The structural determinations show that all  $\text{Au}(\text{PPh}_3)$  groups are non-equivalent in each structure and further, that one of the  $\text{Au}(\text{PPh}_3)$  groups [here labelled Au(3)] is in an environment distinctly different from the other two, which lie over the  $\text{Ru}_3$  triangle in each case. On this

basis, we are inclined to assign the lower field resonances found between  $\delta$  5 and 51 to this group. The closer (stronger) attachment of the  $\text{Au}_3(\text{PPh}_3)_3$  group to one ruthenium [Ru(1)] suggests a possible mode of fluxionality to be rotation of this group about an Ru–Au<sub>3</sub> axis perpendicular to the Au<sub>3</sub> plane. The varying geometries found for the Au<sub>3</sub>/Ru<sub>3</sub> planes reflect only the freezing of this rotational motion in the solid state.

#### 4. Conclusions

Introduction of up to three  $\text{Au}(\text{PR}_3)$  groups onto metal cluster complexes is possible in their reactions with the  $[\text{O}(\text{Au}(\text{PPh}_3))_3]^+$  reagent in the presence of nucleophiles. Hydrido clusters add the  $\text{Au}_3(\text{PR}_3)_3$  unit with concomitant loss of (H + CO). We have also shown that two further  $\text{Au}(\text{PR}_3)$  groups may be added to a cluster already containing a one  $\text{Au}(\text{PR}_3)$  group (but no hydride) to form an  $\text{Au}_3(\text{PR}_3)_3$  unit, with loss of CO. The  $\text{Au}_3(\text{PR}_3)_3$  group contributes three electrons to the cluster valence electron count. The formation of these complexes is driven by the aurophilicity principle [23], that is, the tendency to form Au–Au bonds (but not necessarily the maximum number possible). The resulting  $\text{Au}_3(\text{PR}_3)_3$  group may be open (bent) or closed triangular. In the latter case, the  $\text{Au}_3(\text{PR}_3)_3$  is closely associated with only one of the cluster Ru atoms, although weaker interactions with the other two are also present. In the present group of complexes, we note that clusters of type (a) are found with CO or CR ligands as the only ligands on the cluster, whereas the presence of an unsaturated hydrocarbon results in the type (b) clusters.

The main structural effect of adding an  $\text{Au}_3(\text{PR}_3)_3$  group to the cluster is manifested in an expansion of the average Ru–Ru separation, but little or no significant changes are found in the organic fragments bound to the Ru<sub>3</sub> part of the cluster. However, the average  $\nu(\text{CO})$  frequencies of the aurated clusters are lower than those of the 'parent' derivatives. This feature, together with the cluster expansion, suggests that the aurated clusters are more electron-rich than the 'parents'. The  $\text{Au}_3\text{Ru}_3$  clusters are fluxional as shown by their variable temperature  $^{31}\text{P}$  NMR spectra, while a polyhedral rearrangement process has been suggested for clusters containing type (a)  $\text{Au}_3\text{P}_3$  groups [32], we suggest that for type (b), the rearrangement process could involve rotation of the  $\text{Au}_3\text{P}_3$  group about one Ru atom.

#### 5. Experimental

**Instrumentation:** IR: Perkin-Elmer 1700X FT IR. NMR: Bruker CXP300 or ACP300 ( $^1\text{H}$  NMR at 300.13 MHz,  $^{31}\text{P}$  NMR at 121.49 MHz). FAB MS: VG ZAB

2HF (using 3-nitrobenzyl alcohol as matrix, exciting gas Ar, FAB gun voltage 7.5 kV, current 1 mA, accelerating potential 7 kV).

**General reaction conditions.** Reactions were carried out under an atmosphere of nitrogen, but no special precautions were taken to exclude oxygen during work-up.

**Starting materials.** The following compounds were prepared by procedures identical or similar to those cited:  $\text{Ru}_3(\text{CO})_{12}$  [33],  $\text{Ru}_4(\mu\text{-H})_4(\text{CO})_{12}$  [34],  $\text{Ru}_3(\mu\text{-H})(\mu_3\text{-C}_{12}\text{H}_{15})(\text{CO})_9$  [12],  $\text{Ru}_3(\mu\text{-H})(\mu_3\text{-MeC-CHCMe})(\text{CO})_9$  [35],  $[\text{O}(\text{Au}(\text{PPh}_3))_3][\text{BF}_4]$  [36],  $[\text{ppn}][\text{Co}(\text{CO})_4]$  [37],  $\text{Au}(\text{C}_2\text{Ph})(\text{PPh}_3)$  (R = Ph,  $\text{C}_6\text{H}_4\text{Me-4}$ ) [38],  $\text{Au}(\text{C}_2\text{Bu}^i)(\text{PPh}_3)$  [38], and  $\{\text{Au}(\text{C}_2\text{Ph})_2(\mu\text{-dppe})\}$  [38].

**Preparation of  $\text{Ru}_3(\mu_3\text{-C}_2\text{Ph})(\text{CO})_9\{\text{Au}(\text{PPh}_3)\}$  (9).** To a solution of  $\text{Ru}_3(\text{CO})_{12}$  (135 mg, 0.21 mmol) and  $\text{Au}(\text{C}_2\text{Ph})(\text{PPh}_3)$  (119 mg, 0.21 mmol) in  $\text{CH}_2\text{Cl}_2$  (60 ml) was added  $\text{Me}_3\text{NO}$  (25 mg, 0.33 mmol). The reaction mixture was stirred for 15 min then evaporated to dryness (vacuum line). Radial chromatography (loaded with acetone/light petroleum 1/2, ca. 2 ml) was then performed. Elution with light petroleum gave firstly  $\text{Ru}_3(\text{CO})_{12}$  (15 mg, 11%), then an orange band which was crystallised ( $\text{CH}_2\text{Cl}_2/\text{MeOH}$ ) to give orange-yellow crystals of  $\text{Ru}_3(\mu_3\text{-C}_2\text{Ph})(\text{CO})_9\{\text{Au}(\text{PPh}_3)\}$  (9) (156 mg, 66%) m.p. > 150°C (dec.). Found: C, 37.16; H, 1.79;  $\text{C}_{35}\text{H}_{20}\text{AuO}_9\text{PRu}_3$  requires C, 37.68; H, 1.81%. IR:  $\nu(\text{CO})$  (cyclohexane) 2073w, 2039vs, 1996s, 1990w, 1979(sh), 1966  $\text{cm}^{-1}$ .  $^1\text{H}$  NMR:  $\delta(\text{CDCl}_3)$  7.22–7.57 (m, 20H, Ph). FAB MS ( $m/z$ ): 1117,  $[\text{M}]^+$ , 12; 1089,  $[\text{M-CO}]^+$ , 7; 1061,  $[\text{M-2CO}]^+$ , 4; 1033,  $[\text{M-3CO}]^+$ , 20; 1005,  $[\text{M-4CO}]^+$ , 16; 977,  $[\text{M-5CO}]^+$ , 45; 949,  $[\text{M-6CO}]^+$ , 15; 921,  $[\text{M-7CO}]^+$ , 26; 893,  $[\text{M-8CO}]^+$ , 26; 865,  $[\text{M-9CO}]^+$ , 24; 788,  $[\text{M-9CO-Ph}]^+$ , 20; 721,  $[\text{Au}(\text{PPh}_3)_2]^+$ , 37; 459,  $[\text{Au}(\text{PPh}_3)]^+$ , 100.

**Preparation of  $\text{Ru}_3(\mu_3\text{-C}_2\text{Bu}^i)(\text{CO})_9\{\text{Au}(\text{PPh}_3)\}$  (8).** A similar reaction between  $\text{Ru}_3(\text{CO})_{12}$  (130 mg, 0.20 mmol),  $\text{Au}(\text{C}_2\text{Bu}^i)(\text{PPh}_3)$  (110 mg, 0.20 mmol) and  $\text{Me}_3\text{NO}$  (25 mg, 0.33 mmol) in THF (25 ml) yielded yellow-orange crystals of  $\text{Ru}_3(\mu_3\text{-C}_2\text{Bu}^i)(\text{CO})_9\{\text{Au}(\text{PPh}_3)\}$  (8) (122 mg, 55%). IR (hexane);  $\nu(\text{CO})$  2072m, 2036vs, 1995vs, 1985s, 1978 (sh), 1964  $\text{cm}^{-1}$  [Lit. [14]:  $\nu(\text{CO})$  (hexane) 2074m, 2051s, 2036vs, 1996vs, 1968  $\text{cm}^{-1}$ ].

**Preparation of  $\text{Ru}_3(\mu_3\text{-C}_2\text{Ph})(\text{CO})_9\{\text{Au}[\text{P}(\text{C}_6\text{H}_4\text{Me-4})_3]\}$  (10).** A similar reaction of  $\text{Ru}_3(\text{CO})_{12}$  (37 mg, 0.06 mmol),  $\text{Au}(\text{C}_2\text{Ph})[\text{P}(\text{C}_6\text{H}_4\text{Me-4})_3]$  (35 mg, 0.06 mmol) and  $\text{Me}_3\text{NO}$  (6 mg, 0.08 mmol) in THF (10 ml) yielded yellow-orange crystals of  $\text{Ru}_3(\mu_3\text{-C}_2\text{Ph})(\text{CO})_9\{\text{Au}[\text{P}(\text{C}_6\text{H}_4\text{Me-4})_3]\}$  (10) (39 mg, 58%), m.p. > 150°C (dec.). Found: C, 39.19; H, 2.24;  $\text{C}_{38}\text{H}_{26}\text{AuO}_9\text{PRu}_3$  requires C, 39.42; H, 2.26%. IR:  $\nu(\text{CO})$  (cyclohexane) 2072w, 2038vs, 1996s, 1991(sh), 1978(sh), 1965  $\text{cm}^{-1}$ .  $^1\text{H}$  NMR:  $\delta(\text{CDCl}_3)$  2.40 (s,

9H, Me), 7.20–7.55 (m, 17H, Ph). FAB MS ( $m/z$ ): 1159,  $[M]^+$ , 50; 1131,  $[M-CO]^+$ , 8; 1103,  $[M-2CO]^+$ , 4; 1075,  $[M-3CO]^+$ , 28; 1047,  $[M-4CO]^+$ , 23; 1019,  $[M-5CO]^+$ , 46; 991,  $[M-6CO]^+$ , 15; 963,  $[M-7CO]^+$ , 27; 935,  $[M-8CO]^+$ , 23; 907,  $[M-9CO]^+$ , 22; 805,  $[Au(P(C_6H_4Me)_3)_2]^+$ , 38; 501,  $[Au(P(C_6H_4Me)_3)]^+$ , 100. Strong unidentified peaks at  $m/z$  1539 and 460 were also present.

**Preparation of  $\{Ru_3(\mu_3-C_2Ph)(CO)_9Au\}_2(\mu-dppe)$  (11).** To a stirred solution of  $Ru_3(CO)_{12}$  (100 mg, 0.16 mmol) and  $\{Au(C_2Ph)\}_2dppe$  (119 mg, 0.12 mmol) in  $CH_2Cl_2$  (40 ml) was added  $Me_3NO$  (25 mg, 0.75 mmol). After stirring at room temperature for 0.5 h, preparative TLC (acetone/light petroleum 1/3) showed eight bands and a brown baseline. The major coloured band (yellow–orange,  $R_f$  0.77) was extracted and crystallised from  $CH_2Cl_2/MeOH$  to give yellow–orange crystals of  $\{Ru_3(\mu-C_2Ph)(CO)_9Au\}_2dppe$  (11) (84 mg, 51%), m.p. > 150°C (dec.). Found: C, 33.74; H, 1.59;  $C_{60}H_{34}Au_2O_{18}P_2Ru_6$  requires C, 34.23; H, 1.63%. Infrared (cyclohexane):  $\nu(CO)$  2073w, 2041w, 1966s, 1988(sh), 1962w  $cm^{-1}$ .  $^1H$  NMR:  $\delta(CDCl_3)$  2.74 (s, 4H,  $CH_2$ ), 7.23–7.57 (m, 30H, Ph). FAB MS ( $m/z$ ): 2106,  $[M]^+$ , 45; 1966,  $[M-5CO]^+$ , 23; 1938,  $[M-6CO]^+$ , 72 (the base peak is unidentified at  $m/z$  1392).

### 5.1. Auration reactions using $[O\{Au(PPh_3)\}_3][BF_4]/[ppn][Co(CO)_4]$

(a) **With  $Ru_4(\mu-H)_4(CO)_{12}$ .** To a stirred solution of  $Ru_4(\mu-H)_4(CO)_{12}$  (60 mg, 0.08 mmol) in THF (20 ml) were added  $[O\{Au(PPh_3)\}_3][BF_4]$  (119 mg, 0.08 mmol) and  $[ppn][Co(CO)_4]$  (57 mg, 0.08 mmol) giving a dark red solution. After stirring for 0.5 h the solvent was removed in vacuo. Preparative TLC (benzene/light petroleum 1/1) showed six bands and a brown baseline. Band 1 (yellow,  $R_f$  0.93) was identified as  $Ru_4(\mu-H)_4(CO)_{12}$  (5 mg, 9%) [IR  $\nu(CO)$  spectrum]. Band 3 (orange,  $R_f$  0.77) was crystallised ( $Et_2O$ /light petroleum) to give deep red crystals of  $Ru_4(\mu-H)(\mu-H)_2(CO)_{12}\{Au(PPh_3)\}$  (1) (3 mg, 3%). IR:  $\nu(CO)$  (hexane) 2090m, 2063vs, 2050s, 2030vs, 2012s, 2001m, 1980w, 1965w, 1958w  $cm^{-1}$  [lit. [10]:  $\nu(CO)$  (hexane) 2092s, 2084w, 2066vs, 2052s, 2039(sh), 2032vs, 2015m, 2003(sh), 1982m, 1979m, 1960m, 1900w  $cm^{-1}$ ]. FAB MS ( $m/z$ ): 1204,  $[M]^+$ , 3; 1176,  $[M-CO]^+$ , 4; 1148,  $[M-2CO]^+$ , 5; 1120,  $[M-3CO]^+$ , 9; 1090,  $[M-4CO-2H]^+$ , 9; 1062,  $[M-5CO-2H]^+$ , 8; 1034,  $[M-6CO-2H]^+$ , 22; 1006,  $[M-7CO-2H]^+$ , 9; 978,  $[M-8CO-2H]^+$ , 12; 950,  $[M-9CO-2H]^+$ , 12; 721,  $[Au(PPh_3)_2]^+$ , 34; 459,  $[Au(PPh_3)]^+$ , 100. Band 5 (red–brown,  $R_f$  0.39) was crystallised ( $CH_2Cl_2$ /hexane) to give purple–red crystals of  $Ru_4(\mu_3-H)(\mu-H)(CO)_{12}\{Au_2(PPh_3)_2\}$  (2) (44 mg, 33%). IR:  $\nu(CO)$  ( $CH_2Cl_2$ ) 2071s, 2043m, 2033s, 2023vs, 2008s, 1990m, 1977m, 1959(sh)  $cm^{-1}$  [lit. [27]:  $\nu(CO)$  ( $CH_2Cl_2$ )

2070s, 2043m, 2033s, 2022vs, 2006s, 1988m, 1975m, 1956(sh), 1914(sh)  $cm^{-1}$ ]. FAB MS ( $m/z$ ): 1662,  $[M]^+$ , 4; 1634,  $[M-5CO]^+$ , 3; 1604,  $[M-2CO-2H]^+$ , 7; 1576,  $[M-3CO-2H]^+$ , 6; 1548,  $[M-4CO-2H]^+$ , 6; 1520,  $[M-5CO-2H]^+$ , 13; 1492,  $[M-6CO-2H]^+$ , 5; 1464,  $[M-7CO-2H]^+$ , 5; 1436,  $[M-8CO-2H]^+$ , 5; 1408,  $[M-9CO-2H]^+$ , 8; 1380,  $[M-10CO-2H]^+$ , 6; 1352,  $[M-11CO-2H]^+$ , 7; 1324,  $[M-12CO-2H]^+$ , 5; 721,  $[Au(PPh_3)_2]^+$ , 100; 459,  $[Au(PPh_3)]^+$ , 97. Band 6 (green,  $R_f$  0.20) was crystallised ( $CH_2Cl_2/MeOH$ ) to give green crystals of  $Ru_4(\mu-H)(CO)_{12}\{Au_3(PPh_3)_3\}$  (3) (4 mg, 2%). IR:  $\nu(CO)$  ( $CH_2Cl_2$ ) 2053s, 2012vs, 2009vs, 1989s, 1967m, 1953m, 1919w  $cm^{-1}$  [lit. [9]:  $\nu(CO)$  ( $CH_2Cl_2$ ) 2053vs, 2013(sh), 2007vs, 1989s, 1967w, 1951m, 1920w  $cm^{-1}$ ]. FAB MS ( $m/z$ ): 2120,  $[M]^+$ , 3; 2036,  $[M-3CO]^+$ , 1; 1980,  $[M-5CO]^+$ , 1; 1952,  $[M-6CO]^+$ , 1; 721,  $[Au(PPh_3)_2]^+$ , 100; 459,  $[Au(PPh_3)]^+$ , 92. The remaining bands contained only trace amounts of unidentified products.

(b) **With  $Ru_3(\mu-H)(\mu_3-MeCCHCMe)(CO)_9$ .** Similarly a solution of  $Ru_3(\mu-H)(\mu_3-CMeCHCMe)(CO)_9$  (29 mg, 0.048 mmol) in THF (25 ml) was treated with  $[O\{Au(PPh_3)\}_3][BF_4]$  (72 mg, 0.049 mmol) and  $[ppn][Co(CO)_4]$  (35 mg, 0.049 mmol) to give a red solution. Work-up by preparative TLC (acetone/light petroleum 1/3) gave two major bands. Band 1 (colourless,  $R_f$  0.65) contained  $Co\{Au(PPh_3)\}(CO)_4$  (16 mg, 52%) (spot TLC and solution IR  $\nu(CO)$  spectrum). Band 2 (purple,  $R_f$  0.39) was recrystallised ( $CH_2Cl_2$ /hexane) to give purple–black crystals of  $Ru_3(\mu_3-CMeCHCMe)(CO)_8\{Au_3(PPh_3)_3\}$  (4) (60 mg, 95%), m.p. 220–222°C. Anal. Found: C, 40.59; H, 2.69; M (mass spectrometry), 1973; Calc. for  $C_{67}H_{52}Au_3O_8P_3Ru_3$ : C, 40.80; H, 2.66%; M, 1972. IR:  $\nu(CO)$  ( $CH_2Cl_2$ ) 2042m, 1970s, 1956(sh), 1914w  $cm^{-1}$ .  $^1H$  NMR:  $\delta(CDCl_3)$  2.82 (s, 6H, 2 × Me), 6.33 (s, 1H, CH), 6.94–7.56 (m, 45H, Ph).  $^{31}P$  NMR:  $\delta(CH_2Cl_2)$  62.2 (br) (at 295 K); 45.5 and 62.8 (relative intensities 1:2) (at 245 K). FAB mass spectrum ( $m/z$ ): 1973,  $M^+$ , 1; 1944,  $[M-H-CO]^+$ , 1; 1916,  $[M-H-2CO]^+$ , 10; 721,  $[Au(PPh_3)_2]^+$ , 100; 459,  $[Au(PPh_3)]^+$ , 10.

(c) **With  $Ru_3(\mu-H)(\mu_3-C_{12}H_{15})(CO)_9$ .** To a stirred solution of  $Ru_3(\mu-H)(\mu_3-C_{12}H_{15})(CO)_9$  (42 mg, 0.06 mmol) in THF (15 ml) was added  $[O\{Au(PPh_3)\}_3][BF_4]$  (87 mg, 0.06 mmol) and  $[ppn][Co(CO)_4]$  (42 mg, 0.06 mmol). The colour of the solution changed from yellow to purple within 2 min. After stirring for 5 min the solvent was removed in vacuo. Preparative TLC (acetone/light petroleum 3/7) showed four bands. Band 1 (yellow,  $R_f$  0.90) was identified as  $Ru_3(\mu-H)(\mu_3-C_{12}H_{15})(CO)_9$  [IR  $\nu(CO)$  spectrum] (3 mg, 7%). Band 2 (colourless,  $R_f$  0.68) was identified as  $Co\{Au(PPh_3)\}(CO)_4$  [IR  $\nu(CO)$  spectrum]. Band 3 (red–brown,  $R_f$  0.64) was crystallised (acetone) to give red–brown crystals of  $Ru_3(\mu-H)(\mu_3-C_{12}H_{15})(CO)_8\{Au_2(PPh_3)_2\}$  (5) (57 mg, 60%) m.p. >



150°C (dec.). Found: C, 41.66; H, 2.91;  $C_{56}H_{46}Au_2O_8P_2Ru_3$  requires C, 41.88; H, 2.89%. IR:  $\nu(CO)$  (cyclohexane) 2058m, 2040s, 1988vs, 1981(sh), 1966m, 1915w  $cm^{-1}$ .  $^1H$  NMR:  $\delta(CDCl_3)$  –21.15 [d,  $J(HH) = 2.3Hz$ , 1H, Ru–H], 1.71–5.80 (m, 14H,  $C_{12}$  ring protons), 6.39 [d,  $J(HH) = 2.3Hz$ , 1H, allylic CH], 7.18–7.48 (m, 30H, Ph). FAB MS ( $m/z$ ): 1607,  $[M]^+$ , 3; 1579,  $[M-CO]^+$ , 10; 1551,  $[M-2CO]^+$ , 4; 1522,  $[M-3CO-H]^+$ , 11; 1494,  $[M-4CO-H]^+$ , 23; 1466,  $[M-5CO-H]^+$ , 8; 1438,  $[M-6CO-H]^+$ , 13; 1410,  $[M-7CO-H]^+$ , 20; 1382,  $[M-8CO-H]^+$ , 10; 1251,  $[M-7CO-C_{12}H_{15}-H]^+$ , 7; 1223,  $[M-8CO-C_{12}H_{15}-H]^+$ , 6; 1148,  $[M-Au(PPh_3)]^+$ , 8; 1120,  $[M-CO-Au(PPh_3)]^+$ , 10; 721,  $[Au(PPh_3)_2]^+$ , 100; 459,  $[Au(PPh_3)]^+$ , 48. Band 4 (purple,  $R_f$  0.52) was crystallised from  $CH_2Cl_2/MeOH$  to give thin purple needles of  $Ru_3(\mu_3-C_{12}H_{15})(CO)_8(Au_3(PPh_3)_3)$  (6) (35 mg, 29%). IR:  $\nu(CO)$  (cyclohexane): 2037s, 1975vs, 1954w, 1919m  $cm^{-1}$  [lit. [13]:  $\nu(CO)$  (cyclohexane) 2040m, 1974vs, 1957(sh), 1918m  $cm^{-1}$ ].  $^{31}P\{^1H\}$  NMR:  $\delta(CH_2Cl_2)$  60.3 (br) (at 295 K); 46.2, 61.7, 64.5 (all s, equal intensity; at 245 K).

(d) *With  $Ru_3(\mu_3-C_2Bu')(CO)_6[Au(PPh_3)]$ .* To a stirred solution of  $Ru_3(\mu_3-C_2Bu')(CO)_6[Au(PPh_3)]$  (70 mg, 0.064 mmol) in THF (25 ml) were added  $[O(Au(PPh_3))_3][BF_4]$  (96 mg, 0.065 mmol) and  $[ppn][Co(CO)_4]$  (47 mg, 0.066 mmol) giving an immediate colour change from orange–yellow to orange–brown. After stirring at room temperature for 30 min the solvent was removed (in vacuo). Preparative TLC

Table 4

Non-hydrogen positional and isotropic displacement parameters, (4)

Atom	x	y	z	$U(eq)$ Å <sup>2</sup>
Au(1)	0.44587(6)	0.28895(6)	0.7620(1)	0.0381(4)
Au(2)	0.45235(6)	0.28057(6)	0.5514(1)	0.0437(5)
Au(3)	0.42949(6)	0.16663(6)	0.6653(1)	0.0443(5)
Ru(1)	0.5388(1)	0.2245(1)	0.6711(2)	0.0386(9)
Ru(2)	0.5329(1)	0.3669(1)	0.6516(2)	0.042(1)
Ru(3)	0.5613(1)	0.3132(1)	0.8380(2)	0.044(1)
C(11)	0.540(2)	0.174(2)	0.566(3)	0.07(1)
O(11)	0.549(1)	0.145(1)	0.487(2)	0.084(8)
C(12)	0.534(2)	0.151(2)	0.768(3)	0.07(1)
O(12)	0.540(1)	0.105(1)	0.808(2)	0.060(7)
C(21)	0.471(2)	0.425(2)	0.688(3)	0.06(1)
O(21)	0.434(1)	0.461(1)	0.707(2)	0.083(9)
C(22)	0.532(1)	0.411(2)	0.534(3)	0.05(1)
O(22)	0.538(1)	0.440(1)	0.457(2)	0.081(8)
C(23)	0.593(2)	0.411(2)	0.719(4)	0.12(2)
O(23)	0.628(1)	0.447(1)	0.745(2)	0.083(9)
C(31)	0.507(2)	0.379(2)	0.886(3)	0.06(1)
O(31)	0.484(1)	0.418(1)	0.936(2)	0.088(9)
C(32)	0.625(2)	0.348(2)	0.904(3)	0.07(1)
O(32)	0.661(1)	0.367(1)	0.957(2)	0.089(9)
C(33)	0.548(2)	0.259(2)	0.926(3)	0.08(1)
O(33)	0.538(1)	0.211(1)	0.987(2)	0.078(8)
P(1)	0.3570(4)	0.2941(4)	0.8406(7)	0.045(3)
C(111)	0.345(1)	0.221(1)	0.912(2)	0.043(8)
C(112)	0.394(2)	0.199(2)	0.976(4)	0.12(2)
C(113)	0.389(2)	0.147(2)	1.036(3)	0.08(1)
C(114)	0.339(2)	0.109(2)	1.030(3)	0.08(1)
C(115)	0.326(2)	0.125(2)	0.967(3)	0.08(1)
C(116)	0.235(1)	0.184(2)	0.912(2)	0.052(9)
C(121)	0.285(1)	0.306(1)	0.762(2)	0.045(9)
C(122)	0.257(2)	0.302(2)	0.665(3)	0.07(1)
C(123)	0.246(2)	0.314(2)	0.601(3)	0.09(1)
C(124)	0.195(2)	0.328(2)	0.655(3)	0.08(1)
C(125)	0.187(2)	0.324(2)	0.756(3)	0.09(1)
C(126)	0.237(2)	0.320(2)	0.187(3)	0.08(1)
C(131)	0.349(1)	0.357(1)	0.931(2)	0.043(8)
C(132)	0.349(2)	0.422(2)	0.895(3)	0.07(1)
C(133)	0.342(2)	0.473(2)	0.959(3)	0.07(1)
C(134)	0.336(2)	0.464(2)	1.055(3)	0.08(1)
C(135)	0.330(2)	0.401(2)	1.090(4)	0.11(2)
C(136)	0.336(2)	0.348(2)	1.029(3)	0.08(1)
P(2)	0.4010(4)	0.3042(4)	0.4091(7)	0.048(3)
C(211)	0.354(1)	0.375(1)	0.417(2)	0.049(9)
C(212)	0.373(2)	0.429(2)	0.468(3)	0.06(1)
C(213)	0.336(2)	0.486(2)	0.464(3)	0.07(1)
C(214)	0.285(2)	0.489(2)	0.415(3)	0.08(1)
C(215)	0.265(2)	0.432(2)	0.369(3)	0.10(2)
C(216)	0.298(2)	0.374(2)	0.358(3)	0.09(1)
C(221)	0.355(1)	0.240(1)	0.365(2)	0.044(8)
C(222)	0.330(2)	0.194(2)	0.420(3)	0.07(1)
C(223)	0.288(2)	0.149(2)	0.392(3)	0.06(1)
C(224)	0.277(2)	0.147(2)	0.293(3)	0.07(1)
C(225)	0.297(2)	0.194(2)	0.227(4)	0.10(2)
C(226)	0.340(2)	0.237(2)	0.272(3)	0.07(1)
C(231)	0.448(2)	0.324(2)	0.312(3)	0.06(1)
C(232)	0.492(2)	0.275(2)	0.289(3)	0.07(1)
C(233)	0.536(2)	0.289(2)	0.214(3)	0.09(1)
C(234)	0.531(2)	0.353(2)	0.160(4)	0.11(2)
C(235)	0.494(2)	0.395(2)	0.187(3)	0.06(1)
C(236)	0.448(2)	0.385(2)	0.261(3)	0.06(1)
P(3)	0.3737(4)	0.0730(4)	0.6577(7)	0.046(3)
C(311)	0.413(1)	0.011(2)	0.742(3)	0.051(9)
C(312)	0.431(2)	–0.045(2)	0.700(3)	0.08(1)

Table 3

Crystal data and refinement details for complexes 4 and 13

Compound	4	13
Formula	$C_{67}H_{52}Au_3O_8P_3Ru_3$	$C_{70}H_{50}Au_3O_8P_3Ru_3$ $0.5C_7H_{16}$
MW	1972.2	2056.3
Crystal system	Monoclinic	Triclinic
Space group	$P2_1/n$ (No. 14)	$P\bar{1}$ (No. 2)
a, Å	22.71(4)	21.04(1)
b, Å	20.40(1)	14.323(9)
c, Å	13.69(1)	13.527(8)
$\alpha$ , deg.		99.78(5)
$\beta$ , deg.	90.5(1)	105.23(4)
$\gamma$ , deg.		99.51(5)
V, Å <sup>3</sup>	6341	3781
Z	4	2
$D_c$ , g cm <sup>–3</sup>	2.07	1.81
$F(000)$	3568	1954
Crystal size, mm	$0.30 \times 0.33 \times 0.20$	$0.08 \times 0.33 \times 0.16$
$A^\circ$ (min, max)	3.32, 8.1	1.56, 3.69
$\mu$ , cm <sup>–1</sup>	74	62
$2\theta_{max}$ , deg.	50	50
N	11116	13282
$N_o$	6045	8875
R	0.087	0.045
$R_w$	0.090	0.057

Table 4 (continued)

Atom	<i>x</i>	<i>y</i>	<i>z</i>	<i>U</i> (eq) Å <sup>2</sup>
C(313)	0.458(2)	−0.088(2)	0.765(4)	0.10(1)
C(314)	0.456(2)	−0.070(2)	0.862(3)	0.09(1)
C(315)	0.435(2)	−0.018(2)	0.914(4)	0.11(2)
C(316)	0.413(2)	0.031(2)	0.838(3)	0.06(1)
C(321)	0.299(2)	0.075(2)	0.700(3)	0.06(1)
C(322)	0.270(2)	0.025(2)	0.753(3)	0.09(1)
C(323)	0.216(2)	0.027(2)	0.790(3)	0.07(1)
C(324)	0.182(2)	0.079(2)	0.759(3)	0.07(1)
C(325)	0.204(2)	0.129(2)	0.711(3)	0.07(1)
C(326)	0.265(2)	0.128(2)	0.676(3)	0.06(1)
C(331)	0.372(2)	0.035(2)	0.533(3)	0.06(1)
C(332)	0.417(2)	0.047(2)	0.473(3)	0.06(1)
C(333)	0.416(2)	0.014(2)	0.387(3)	0.08(1)
C(334)	0.370(3)	−0.026(3)	0.352(4)	0.13(2)
C(335)	0.327(2)	−0.038(2)	0.426(4)	0.09(1)
C(336)	0.327(2)	−0.009(3)	0.517(4)	0.12(2)
C(1)	0.610(2)	0.300(2)	0.491(3)	0.08(1)
C(2)	0.594(2)	0.304(2)	0.600(3)	0.06(1)
C(3)	0.630(1)	0.264(1)	0.659(3)	0.052(9)
C(4)	0.617(1)	0.250(1)	0.758(2)	0.046(9)
C(5)	0.659(2)	0.204(2)	0.815(3)	0.09(1)

(acetone/light petroleum 15/85) showed two major bands. Band 1 (colourless,  $R_f$  0.73) was identified as  $\text{Co}\{\text{Au}(\text{PPh}_3)\}(\text{CO})_4$  (spot TLC and solution IR). Band 2 (orange,  $R_f$  0.58) was crystallised from  $\text{CH}_2\text{Cl}_2$ /n-heptane to give orange crystals of  $\text{Ru}_3(\mu_3\text{-C}_2\text{Bu})(\text{CO})_8[\text{Au}_3(\text{PPh}_3)_3]$  (**12**) (94 mg, 74%). Anal. Found: M (mass spectrometry), 1987; calcd. M, 1987. Infrared (cyclohexane):  $\nu(\text{CO})$  2045vs, 2016vs, 1978s, 1965sh, 1961s, 1953sh, 1908w  $\text{cm}^{-1}$ .  $^1\text{H}$  NMR:  $\delta(\text{CDCl}_3)$  1.50 (s, 9 H,  $^t\text{Bu}$ ), 6.98–7.56 (m, 45 H, Ph). [Lit. [15]:  $\nu(\text{CO})$  2048vs, 2018vs, 1982s, 1971m, 1964s, 1956w, 1912m  $\text{cm}^{-1}$ .  $^1\text{H}$  NMR:  $\delta(\text{CDCl}_3)$  1.50 (s, 9 H,  $^t\text{Bu}$ ), 7.44 (m, 45 H, Ph)].

(e) With  $\text{Ru}_3(\mu_3\text{-C}_2\text{Ph})(\text{CO})_9[\text{Au}(\text{PPh}_3)]$ . To a stirred solution of  $\text{Ru}_3(\mu_3\text{-C}_2\text{Ph})(\text{CO})_9[\text{Au}(\text{PPh}_3)]$  (50 mg, 0.045 mmol) in THF (15 ml) were added  $[\text{O}(\text{Au}(\text{PPh}_3))_3][\text{BF}_4]$  (67 mg, 0.045 mmol) and  $[\text{ppn}][\text{Co}(\text{CO})_4]$  (32 mg, 0.045 mmol) the colour of the solution immediately changing from yellow to orange. After stirring at room temperature for 10 min the solvent was removed in vacuo. Preparative TLC (acetone/light petroleum 3/7) showed four bands. Band 2 (colourless,  $R_f$  0.53) was identified as  $\text{Co}\{\text{Au}(\text{PPh}_3)\}(\text{CO})_4$  (spot TLC). Band 3 (orange,  $R_f$  0.47) was crystallised ( $\text{CH}_2\text{Cl}_2$ /n-heptane) to give orange crystals of  $\text{Ru}_3(\mu_3\text{-C}_2\text{Ph})(\text{CO})_8[\text{Au}_3(\text{PPh}_3)_3]$  (**13**) (67 mg, 75%), m.p. > 150°C (dec.). Found: C, 42.35; H, 2.82;  $\text{C}_{70}\text{H}_{50}\text{Au}_3\text{O}_8\text{P}_3\text{Ru}_3$  requires C, 41.91; H, 2.51%. IR  $\nu(\text{CO})$  (cyclohexane) 2047vs, 2020vs, 1981s, 1968sh, 1965s, 1950sh, 1914w  $\text{cm}^{-1}$ .  $^1\text{H}$  NMR:  $\delta(\text{CDCl}_3)$  6.99–7.57 (m, Ph).  $^{31}\text{P}\{^1\text{H}\}$  NMR:  $\delta(\text{CH}_2\text{Cl}_2)$  56.7 (br) (at 295 K); 51.7, 56.7, 65.3 (all s, equal intensity; at 255 K). FAB MS ( $m/z$ ): 2466,

Table 5

Non-hydrogen coordinates and isotropic thermal parameters, (13)

Atom	<i>x</i>	<i>y</i>	<i>z</i>	<i>U</i> (eq) Å <sup>2</sup>
Au(1)	0.18199(3)	0.28291(4)	0.19853(4)	0.0428(2)
Au(2)	0.21490(3)	0.23539(4)	0.40424(4)	0.0452(3)
Au(3)	0.28106(3)	0.41500(4)	0.36795(5)	0.0509(3)
Ru(1)	0.30049(6)	0.23781(8)	0.28893(9)	0.0433(5)
Ru(2)	0.25260(6)	0.05723(8)	0.32307(9)	0.0497(6)
Ru(3)	0.19390(6)	0.08952(8)	0.12052(9)	0.0518(6)
C(11)	0.3699(7)	0.294(1)	0.413(1)	0.058(7)
O(11)	0.4138(6)	0.3225(9)	0.4885(9)	0.110(8)
C(12)	0.3348(7)	0.310(1)	0.201(1)	0.055(7)
O(12)	0.3533(6)	0.3516(8)	0.1481(9)	0.086(7)
C(21)	0.1667(7)	0.0340(9)	0.341(1)	0.058(7)
O(21)	0.1149(5)	0.0057(7)	0.3499(8)	0.078(6)
C(22)	0.3027(8)	0.072(1)	0.465(1)	0.071(9)
O(22)	0.3333(6)	0.079(1)	0.5486(9)	0.109(8)
C(23)	0.254(1)	−0.074(1)	0.281(1)	0.10(1)
O(23)	0.2553(8)	−0.1524(8)	0.254(1)	0.125(9)
C(31)	0.1023(7)	0.085(1)	0.120(1)	0.057(7)
O(31)	0.0463(5)	0.0725(8)	0.1208(8)	0.081(6)
C(32)	0.1712(9)	−0.040(1)	0.042(1)	0.081(9)
O(32)	0.1598(7)	−0.1171(9)	−0.008(1)	0.121(8)
C(33)	0.1908(8)	0.152(1)	0.004(1)	0.072(9)
O(33)	0.1908(8)	0.185(1)	−0.0639(8)	0.118(9)
P(1)	0.1089(2)	0.3707(3)	0.1209(3)	0.046(2)
C(111)	0.1551(7)	0.4826(9)	0.107(1)	0.048(7)
C(112)	0.2228(9)	0.488(1)	0.103(1)	0.069(8)
C(113)	0.2605(9)	0.571(1)	0.091(1)	0.077(9)
C(114)	0.2323(9)	0.649(1)	0.081(1)	0.081(9)
C(115)	0.1679(9)	0.647(1)	0.087(1)	0.083(9)
C(116)	0.1305(7)	0.563(1)	0.099(1)	0.061(8)
C(121)	0.0524(7)	0.4120(9)	0.192(1)	0.051(7)
C(122)	0.0792(7)	0.443(1)	0.298(1)	0.054(7)
C(123)	0.030(1)	0.479(1)	0.349(1)	0.09(1)
C(124)	−0.0337(9)	0.475(1)	0.297(2)	0.09(1)
C(125)	−0.0568(9)	0.441(1)	0.194(1)	0.09(1)
C(126)	−0.0150(9)	0.412(1)	0.141(1)	0.08(1)
C(131)	0.0560(7)	0.3116(9)	−0.013(1)	0.048(7)
C(132)	0.0060(9)	0.229(1)	−0.033(1)	0.09(1)
C(133)	−0.0288(9)	0.181(1)	−0.130(1)	0.09(1)
C(134)	−0.0225(7)	0.211(1)	−0.214(1)	0.070(8)
C(135)	0.024(1)	0.292(1)	−0.197(1)	0.14(1)
C(136)	0.066(1)	0.345(1)	−0.097(1)	0.10(1)
P(2)	0.1480(2)	0.2521(3)	0.5131(3)	0.051(2)
C(211)	0.0593(7)	0.253(1)	0.446(1)	0.050(7)
C(212)	0.0358(7)	0.214(1)	0.339(1)	0.054(7)
C(213)	−0.028(1)	0.210(1)	0.284(1)	0.09(1)
C(214)	−0.0743(8)	0.246(1)	0.333(1)	0.079(9)
C(215)	−0.0494(9)	0.285(1)	0.441(1)	0.09(1)
C(216)	0.0194(9)	0.290(1)	0.499(1)	0.077(9)
C(221)	0.1777(7)	0.360(1)	0.618(1)	0.056(7)
C(222)	0.1861(9)	0.450(1)	0.590(1)	0.077(9)
C(223)	0.211(1)	0.536(1)	0.665(1)	0.09(1)
C(224)	0.222(1)	0.533(1)	0.767(2)	0.12(1)
C(225)	0.212(1)	0.447(1)	0.798(1)	0.10(1)
C(226)	0.1899(9)	0.359(1)	0.722(1)	0.079(9)
C(231)	0.1422(9)	0.155(1)	0.583(1)	0.064(8)
C(232)	0.2032(8)	0.126(1)	0.624(1)	0.079(9)
C(233)	0.207(1)	0.056(1)	0.681(1)	0.11(1)
C(234)	0.141(1)	0.010(1)	0.690(1)	0.11(1)
C(235)	0.082(1)	0.033(1)	0.642(2)	0.13(1)
C(236)	0.0831(9)	0.100(1)	0.591(1)	0.09(1)
P(3)	0.3258(2)	0.5751(3)	0.4469(3)	0.053(2)
C(311)	0.3770(7)	0.633(1)	0.375(1)	0.060(7)

Table 5 (continued)

Atom	<i>x</i>	<i>y</i>	<i>z</i>	<i>U</i> (eq) Å <sup>2</sup>
C(312)	0.3692(9)	0.723(1)	0.353(1)	0.09(1)
C(313)	0.417(1)	0.765(2)	0.305(2)	0.13(2)
C(314)	0.4559(9)	0.716(2)	0.268(2)	0.11(1)
C(315)	0.463(1)	0.626(2)	0.286(2)	0.12(1)
C(316)	0.4185(9)	0.581(1)	0.339(2)	0.10(1)
C(321)	0.2709(6)	0.6605(9)	0.465(1)	0.047(6)
C(322)	0.2878(8)	0.736(1)	0.551(1)	0.079(9)
C(323)	0.253(1)	0.804(1)	0.558(1)	0.10(1)
C(324)	0.1921(9)	0.794(1)	0.478(1)	0.08(1)
C(325)	0.1721(7)	0.718(1)	0.390(1)	0.08(1)
C(326)	0.2162(8)	0.651(1)	0.388(1)	0.073(9)
C(331)	0.3865(7)	0.588(1)	0.575(1)	0.057(7)
C(332)	0.3676(9)	0.525(1)	0.634(1)	0.09(1)
C(333)	0.412(1)	0.533(1)	0.737(1)	0.11(1)
C(334)	0.470(1)	0.604(2)	0.773(1)	0.13(1)
C(335)	0.4868(8)	0.669(1)	0.716(1)	0.10(1)
C(336)	0.444(1)	0.659(1)	0.617(1)	0.09(1)
C(1)	0.2883(7)	0.0962(9)	0.193(1)	0.055(7)
C(2)	0.3418(7)	0.1069(9)	0.273(1)	0.052(7)
C(101)	0.4099(7)	0.0854(9)	0.295(1)	0.050(7)
C(102)	0.4532(9)	0.099(1)	0.396(1)	0.08(1)
C(103)	0.5160(8)	0.076(1)	0.408(1)	0.09(1)
C(104)	0.537(1)	0.039(2)	0.330(2)	0.11(1)
C(105)	0.497(1)	0.028(2)	0.235(2)	0.15(2)
C(106)	0.429(1)	0.050(2)	0.214(1)	0.13(1)
C(01) <sup>a</sup>	0.35(1)	0.262(6)	−0.12(1)	0.14(2)
C(02) <sup>a</sup>	0.415(8)	0.187(3)	−0.072(6)	0.16(2)
C(03) <sup>a</sup>	0.380(4)	0.098(2)	−0.099(3)	0.29(4)
C(04) <sup>a</sup>	0.371(2)	0.052(2)	−0.061(2)	0.49(8)
C(05) <sup>a</sup>	0.332(4)	−0.048(3)	−0.112(3)	0.19(2)
C(06) <sup>a</sup>	0.32(1)	−0.168(2)	−0.115(8)	0.15(2)
C(07) <sup>a</sup>	0.37(1)	−0.172(6)	−0.04(1)	0.22(3)

<sup>a</sup>Atom refined with isotropic thermal parameters.

[M + Au(PPh<sub>3</sub>)<sub>3</sub>]<sup>+</sup> ≡ [M']<sup>+</sup>, 1; 2438, [M'−CO]<sup>+</sup>, 1; 2410, [M'−2CO]<sup>+</sup>, 3; 2092, [M'−PPh<sub>3</sub>−4CO]<sup>+</sup>, 1; 2064, [M'−PPh<sub>3</sub>−5 CO]<sup>+</sup>, 2; 2036, [M'−PPh<sub>3</sub>−6CO]<sup>+</sup>, 2; 2007, [M]<sup>+</sup>, 3; 1979, [M−CO]<sup>+</sup>, 4; 1895, [M−4CO]<sup>+</sup>, 8; 1839, [M−6CO]<sup>+</sup>, 4; 1811, [M−7CO]<sup>+</sup>, 3; 1783, [M−8CO]<sup>+</sup>, 3; 1745, [M−PPh<sub>3</sub>]<sup>+</sup>, 3; 1717, [M−PPh<sub>3</sub>−CO]<sup>+</sup>, 4; 1548, [M−Au(PPh<sub>3</sub>)<sub>3</sub>]<sup>+</sup>, 5; 1520, [M−Au(PPh<sub>3</sub>)<sub>3</sub>−CO]<sup>+</sup>, 19; 721, [Au(PPh<sub>3</sub>)<sub>2</sub>]<sup>+</sup>, 100; 459, [Au(PPh<sub>3</sub>)<sub>3</sub>]<sup>+</sup>, 92.

## 6. Crystallography

Unique data sets were measured at ca. 295 K within the specified  $2\theta_{\max}$  limits using an Enraf–Nonius CAD4 diffractometer ( $2\theta/\theta$  scan mode; monochromatic Mo-K  $\alpha$  radiation,  $\lambda$  0.71073 Å); *N* independent reflections were obtained,  $N_0$  with  $I > 3\sigma(I)$  being considered 'observed' and used in the full matrix least squares refinement after analytical absorption correction. Anisotropic thermal parameters were refined for Au, Ru and P in **4**, and all non-hydrogen atoms in **13**; (*x*, *y*, *z*,  $U_{\text{iso}}$ )<sub>H</sub> were included constrained at estimated values. Conventional residuals *R*, *R'* on  $|F|$  are quoted, statisti-

cal weights derivative of  $\sigma^2(I) = \sigma^2(I_{\text{diff}}) + 0.0004\sigma^4(I_{\text{diff}})$  being used. Computation used the XTAL 3.0 program system [39] implemented by S.R. Hall; neutral atom complex scattering factors were employed. Pertinent results are given in the Figs. and Tables 1–5; material deposited comprises thermal and hydrogen parameters and full molecular non-hydrogen geometries.

### 6.1. Abnormal features / variations in procedure

(4) Weak data with wide linewidths from a poor quality specimen would only support meaningful anisotropic thermal parameter refinement for Au, Ru, P, the isotropic form being used for O, N, C.

(13) Difference map residues were modelled as an *n*-heptane solvent molecule, site occupancy set at 0.5 after trial refinement.

## Acknowledgements

Financial support from the Australian Research Council is gratefully acknowledged. PAH held a University of Adelaide postgraduate Research Scholarship. We thank Johnson Matthey Technology for a generous loan of RuCl<sub>3</sub> · *n*H<sub>2</sub>O.

## References

- [1] M.I. Bruce, E. Horn, P.A. Humphrey, E.R.T. Tiekink, *J. Organomet. Chem.* 518 (1996) 121.
- [2] D.M.P. Mingos, M.J. Watson, *Adv. Inorg. Chem.* 39 (1992) 378.
- [3] (a) L.W. Bateman, M. Green, J.A.K. Howard, K.A. Mead, R.M. Mills, I.D. Salter, F.G.A. Stone, P. Woodward, *J. Chem. Soc., Chem. Commun.* (1982) 773. (b) L.W. Bateman, M. Green, K.A. Mead, R.M. Mills, I.D. Salter, F.G.A. Stone, P. Woodward, *J. Chem. Soc., Dalton Trans.* (1983) 2599.
- [4] J.E. Ellis, *J. Am. Chem. Soc.* 103 (1981) 6106.
- [5] (a) M.I. Bruce, B.K. Nicholson, *J. Chem. Soc., Chem. Commun.* (1982) 1141. (b) K.S. Harpp, C.E. Housecroft, A.L. Rheingold, M.S. Shongwe, *J. Chem. Soc., Chem. Commun.* (1988) 965.
- [6] P.D. Boyle, B.J. Johnson, A. Buehler, L.M. Pignolet, *Inorg. Chem.* 25 (1986) 5.
- [7] M.I. Bruce, P.E. Corbin, P.A. Humphrey, G.A. Koutsantonis, M.J. Liddell, E.R.T. Tiekink, *J. Chem. Soc., Chem. Commun.* (1990) 674.
- [8] (a) T. Blumenthal, M.I. Bruce, O. bin Shawkataly, B.N. Green, I. Lewis, *J. Organomet. Chem.* 269 (1984) C10; (b) M.I. Bruce, M.J. Liddell, *J. Organomet. Chem.* 427 (1992) 263.
- [9] J.A.K. Howard, I.D. Salter, F.G.A. Stone, *Polyhedron* 3 (1984) 567.
- [10] M.I. Bruce, B.K. Nicholson, *J. Organomet. Chem.* 252 (1983) 243.
- [11] S. Aime, L. Milone, D. Osella, M. Valle, *J. Chem. Res.* (1978) (S) 77, (M) 785.

- [12] M.I. Bruce, M.A. Cairns, M. Green, *J. Chem. Soc., Dalton Trans.* (1972) 1293.
- [13] M.I. Bruce, O. bin Shawkataly, B.K. Nicholson, *J. Organomet. Chem.* 275 (1984) 223.
- [14] P. Braunstein, G. Predieri, A. Tiripicchio, E. Sappa, *Inorg. Chim. Acta* 63 (1982) 113.
- [15] M.I. Bruce, E. Horn, O. bin Shawkataly, M.R. Snow, *J. Organomet. Chem.* 280 (1985) 289.
- [16] V. Dearing, S.R. Drake, B.F.G. Johnson, J. Lewis, M. McPartlin, H.R. Powell, *J. Chem. Soc., Chem. Commun.* (1988) 1331.
- [17] (a) B.F.G. Johnson, J. Lewis, A.G. Orpen, P.R. Raithby, G. Süss, *J. Organomet. Chem.* 173 (1979) 187; (b) M.R. Churchill, L.R. Beanan, H.J. Wasserman, C. Bueno, Z. Abdul Rahman, J.B. Keister, *Organometallics* 2 (1983) 1179.
- [18] A. Cox, P. Woodward, *J. Chem. Soc. (A)* (1971) 3599.
- [19] M. Catti, G. Gervasio, S.A. Mason, *J. Chem. Soc., Dalton Trans.* (1977) 2260.
- [20] M.R. Churchill, L.A. Buttrey, J.B. Keister, J.W. Ziller, T.S. Janik, W.S. Striejewske, *Organometallics* 9 (1990) 766.
- [21] T. Adatia, M. McPartlin, I.D. Salter, *J. Chem. Soc., Dalton Trans.* (1988) 751.
- [22] W.B. Pearson, *Lattice Spacings and Structures of Metals and Alloys*, Pergamon Press, London, 1951.
- [23] H. Schmidbaur, *Gold Bull.* 23 (1990) 11; *Interdisc. Sci. Rev.* 17 (1992) 213; *Chem. Soc. Rev.* 24 (1995) 391.
- [24] J.W. Lauher, K. Wald, *J. Am. Chem. Soc.* 103 (1981) 7648.
- [25] (a) R.D. Wilson, S.M. Wu, R.A. Love, R. Bau, *Inorg. Chem.* 17 (1978) 1271; (b) J. Evans, A.C. Street, M. Webster, *Organometallics* 6 (1987) 794.
- [26] K. Henrick, B.F.G. Johnson, J. Lewis, J. Mace, M. McPartlin, J. Morris, *J. Chem. Soc., Chem. Commun.* (1985) 1617.
- [27] M.J. Freeman, A.G. Orpen, I.D. Salter, *J. Chem. Soc., Dalton Trans.* (1987) 379.
- [28] G.J. Kubas, R.R. Ryan, B.I. Swanson, P.J. Vergamini, H.J. Wasserman, *J. Am. Chem. Soc.* 106 (1984) 451. See also the recent reviews: (a) D.M. Heinekey, *Chem. Rev.* 93 (1993) 913; (b) R.H. Morris, P.G. Jessop, *Coord. Chem. Rev.* 121 (1992) 155; (c) A. Dedieu (Ed.), *Transition Metal Hydrides*, VCH, Weinheim, 1991.
- [29] T. Oka, *Phys. Rev. Lett.* 45 (1980) 531.
- [30] (a) J.K. Burdett, J.R. Phillips, M.R. Pourian, M. Poliakoff, J.J. Turner, R. Upmaces, *Inorg. Chem.* 26 (1987) 3054; (b) G. Pacchioni, *J. Am. Chem. Soc.* 112 (1990) 80.
- [31] B.R. Sutherland, K. Folting, W.E. Streib, D.M. Ho, J.C. Huffman, K.G. Caulton, *J. Am. Chem. Soc.* 109 (1987) 3489.
- [32] A.G. Orpen, I.D. Salter, *Organometallics* 10 (1991) 111.
- [33] M.I. Bruce, C.M. Jensen, N.L. Jones, *Inorg. Synth.* 26 (1989) 259; 28 (1990) 216.
- [34] M.I. Bruce, M.L. Williams, *Inorg. Synth.* 26 (1989) 262; 28 (1990) 219.
- [35] S. Aime, D. Osella, *Organomet. Synth.* 4 (1988) 253.
- [36] M.I. Bruce, B.K. Nicholson, O. bin Shawkataly, *Inorg. Synth.* 26 (1989) 326.
- [37] J.K. Ruff, W.J. Schlientz, *Inorg. Synth.* 15 (1974) 84.
- [38] R.J. Cross, M.F. Davidson, *J. Chem. Soc., Dalton Trans.* (1986) 411.
- [39] S.R. Hall, J.M. Stewart (Eds.), *XTAL Users' Manual*, Version 3.0, Universities of Western Australia and Maryland, 1990.